A R C H I V E O F M E C H A N I C A L E N G I N E E R I N G

VOL. LXI 2014 Number 2

10.2478/meceng-2014-0019

Key words: single-axle mobile robot, nonholonomic constraints, Hamel's equation, cascade control structure, input-output linearization, tracking control, nonlinear control

TOBIAS ZAICZEK [*], *MATTHIAS FRANKE* [**]

TRACKING CONTROL OF A BALANCING ROBOT – A MODEL-BASED APPROACH

This paper presents a control concept for a single-axle mobile robot moving on the horizontal plane. A mathematical model of the nonholonomic mechanical system is derived using Hamel's equations of motion. Subsequently, a concept for a tracking controller is described in detail. This controller keeps the mobile robot on a given reference trajectory while maintaining it in an upright position. The control objective is reached by a cascade control structure. By an appropriate input transformation, we are able to utilize an input-output linearization of a subsystem. For the remaining dynamics a linear set-point control law is presented. Finally, the performance of the implemented control law is illustrated by simulation results.

1. Introduction

In industrial as well as in transport and service applications, single-axle mobile robots can be used profitably. In comparison to traditional vehicles, their main advantages are their smaller size and lower production costs. During the last years, mobile robots have received increasing attention with respect to their modeling and controller design. The main difficulties in the design process are due to the nonholonomic constraints combined with the inherent instability of the system [1, 2, 3, 4, 5, 6, 7].

In this paper, we consider a single-axle mobile robot as illustrated in Figure 1. It consists of a main body with an axle at its bottom and is equipped with two independently driven wheels, each attached to one end of the axle. This vehicle drives without slip on a horizontal plane. This means, we investigate a mechanical system that is subject to nonholonomic constraints.

[*] *Fraunhofer-Institute Integrated Circuits, Design Automation Division, Zeunerstraße 38, 01069 Dresden, Germany; E-mail: tobias.zaiczek@eas.iis.fraunhofer.de*

[**] *Fraunhofer-Institute Integrated Circuits, Design Automation Division, Zeunerstraße 38, 01069 Dresden, Germany; E-mail: matthias.franke@eas.iis.fraunhofer.de*

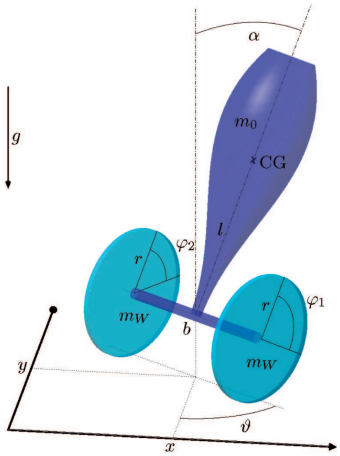

Fig. 1. Mobile robot rolling on the horizontal plane. The wheels are assumed to be ideal disks. The center of gravity of the main body is labeled by CG. Its distance from the wheels' axle is l

One way of dealing with this type of mechanical systems is utilizing Lagrange multipliers to represent the reaction forces of the constraints, see e.g. [8, 9]. This approach leads to a system of differential algebraic equations, whose solution is more involved than the solution of ordinary differential equations (ODE-system), see [10, 11, 12, 13]. Moreover, the dimension of the problem is higher compared to the original system since the Lagrange multipliers appear in the equations.

In Section 2, we follow another approach for the derivation of the equations of motion that is ascribed to Hamel [1]. His approach can directly take into account the nonholonomic constraints and results in a system of ordinary differential equations of lowest possible dimension. Within the literature, one can find contributions on other mechanical systems where this approach has already been proven beneficial [9, 14, 15].

The second part of the paper comprises a control concept for the mobile robot which is able to meet both requirements: first, to keep the main body upright, and second, to maintain the position of the axle's center point close to a reference trajectory. Both tasks are accomplished by a cascade control structure that is described in section 3.

Section 4 finally presents some simulation results to illustrate the controller's performance on the derived mathematical model.

2. Modeling

We consider a single-axle mobile robot with two independently driven wheels rolling on a horizontal plane as illustrated in Figure 1. The body of

the robot as well as each of the wheels are assumed to be rigid. The position of the center of the axle can be expressed in terms of the coordinates x and y, whereas the wheels' angles with respect to the main body are described by φ_1 and φ_2. Furthermore, the angles ϑ and α denote the rotation of the robot's body around the vertical axis and, respectively, the wheels' axis. The wheels' radius and the length of the axle are designated by the constants r and b, respectively. Moreover, the y-axis of the global coordinate system is defined to be parallel to the robot's axle for $\vartheta = 0$. The gravitational field acts in vertical direction with gravity constant g. If $\alpha = 0$ and $\vartheta = 0$ the principal axes of inertia of the main body are supposed to be parallel to the axes of the global coordinate system. The corresponding principal moments of inertia of this body w. r. t. its center of mass are J_x, J_y, and J_z, while the wheels are assumed to be ideal disks with principal moments of inertia $\frac{1}{2}m_w r^2$ and $\frac{1}{4}m_w r^2$, respectively. The distance between the center of gravity of the main body and the wheels' common axis is denoted by l. In order to manipulate the robot, the torques τ_1 and τ_2 can be applied between the body and the right and left wheel, respectively.

2.1. Kinematic Description of the Rolling Robot

The configuration of the rolling robot may be described in terms of the six positional coordinates

$$q_0 = \vartheta, \quad q_1 = x, \quad q_2 = y, \quad q_3 = \varphi_1, \quad q_4 = \varphi_2 \quad \text{and} \quad q_5 = \alpha. \tag{1}$$

For the kinematic description of the rolling robot it has proven beneficial to introduce the following six quasi-velocities

$$\begin{aligned} \omega_0 &= b\dot{\vartheta} - r(\dot{\varphi}_1 - \dot{\varphi}_2) & \omega_1 &= \dot{x}\sin\vartheta - \dot{y}\cos\vartheta, \\ \omega_2 &= r\dot{\alpha} + \frac{r}{2}(\dot{\varphi}_1 + \dot{\varphi}_2) - (\dot{x}\cos\vartheta + \dot{y}\sin\vartheta), & \omega_3 &= \dot{\alpha}, \\ \omega_4 &= \dot{x}\cos\vartheta + \dot{y}\sin\vartheta, & \omega_5 &= \frac{r}{b}(\dot{\varphi}_1 - \dot{\varphi}_2). \end{aligned} \tag{2}$$

In order to give an illustrative meaning for these variables, ω_1 can be interpreted as the velocity of the axle's center point in the direction of the wheels' axis and ω_4 as its (nonholonomic) path velocity v. Concerning the movement of the axle's center point, the velocity coordinate ω_2 gives a measure for the slip of the wheels when driving straight ahead, whereas ω_0 refers to slip when turning around its vertical axis. Moreover, ω_3 and ω_5 represent the angular velocities of the main body around the wheels' axis and the vertical line, respectively.

Since, for the vehicle's wheels, slipping should not be permitted in both, the driving direction and in lateral direction, the velocities ω_0, ω_1 and ω_2 must vanish identically. While the constraint equation $\omega_0 = 0$ is holonomic, the remaining conditions result in the following nonholonomic constraints:

$$\omega_1 = \dot{x}\sin\vartheta - \dot{y}\cos\vartheta = 0, \quad \omega_2 = r\dot{\alpha} + \frac{r}{2}(\dot{\varphi}_1 + \dot{\varphi}_2) - (\dot{x}\cos\vartheta + \dot{y}\sin\vartheta) = 0. \tag{3}$$

In fact the constraint equation $\omega_0 = 0$ can easily be integrated with respect to time yielding

$$\vartheta = \frac{r}{b}(\varphi_1 - \varphi_2) + \vartheta_0 \tag{4}$$

with some arbitrary integration constant ϑ_0 being set to zero for the remainder of this paper. Regarding this condition as given, we can now reduce the complexity of the kinematic description and drop the coordinates q_0 and ω_0. Since we cannot further reduce the number of coordinates, the dimension of the configuration space equals five.

Note, that the definition of ω_3 to ω_5 was not made arbitrarily but in a way to get an invertible transformation between the velocity coordinates ω_i and the time derivatives $\dot{q}_j$ for $i, j = 1, \ldots, 5$. The inverse transformation can thus be stated as

$$\begin{aligned}
\dot{x} &= \sin\left(r\frac{\varphi_1 - \varphi_2}{b}\right)\omega_1 + \cos\left(r\frac{\varphi_1 - \varphi_2}{b}\right)\omega_4, & \dot{\varphi}_1 &= \frac{1}{r}\omega_2 - \omega_3 + \frac{1}{r}\omega_4 + \frac{b}{2r}\omega_5,\\
\dot{y} &= -\cos\left(r\frac{\varphi_1 - \varphi_2}{b}\right)\omega_1 + \sin\left(r\frac{\varphi_1 - \varphi_2}{b}\right)\omega_4, & \dot{\varphi}_2 &= \frac{1}{r}\omega_2 - \omega_3 + \frac{1}{r}\omega_4 - \frac{b}{2r}\omega_5,\\
\dot{\alpha} &= \omega_3.
\end{aligned} \tag{5}$$

2.2. Equations of Motion of the rolling robot

In this subsection the equations of motion will be derived using Hamel's Equations [1]. His approach allows us to directly take the given nonholonomic constraints into account, which – compared to other approaches – reduces the numerical complexity significantly (refer to [7]).

For that, we first have to express the kinetic energy in terms of the introduced velocity coordinates ω_i ($i = 1, \ldots, 5$)) without prior consideration of the nonholonomic constraints (3). One hence gets

$$T = \frac{m_0 + 2m_w}{2}\omega_1^2 + \frac{m_w}{2}\omega_2^2 + \frac{J_y + m_0 l^2}{2}\omega_3^2 + \frac{m_0 + 3m_w}{2}\omega_4^2 + \\ + \frac{J_5}{2}\omega_5^2 + m_0 l(\omega_3\omega_4 \cos\alpha - \omega_1\omega_5 \sin\alpha) - m_w\omega_2\omega_4 \tag{6}$$

where m_0, m_w are the masses of the body and one wheel, respectively. The moment of inertia J_5 is defined by

$$J_5 = (J_x + m_0 l^2)\sin^2\alpha + J_z \cos^2\alpha + \frac{3}{4}m_w b^2 + \frac{1}{2}m_w r^2. \tag{7}$$

The potential energy is simply given by

$$U = -m_0 l g \cos\alpha. \tag{8}$$

Hamel's equations of motion [1] can be generally expressed as

$$\frac{d}{dt}\frac{\partial T}{\partial \omega_k} - \sum_{j=1}^{n}\left(\frac{\partial T}{\partial q_j} - \frac{\partial U}{\partial q_j}\right)\frac{\partial \dot{q}_j(\omega)}{\partial \omega_k} + \sum_{j=1}^{n}\sum_{l=p+1}^{n}\frac{\partial T}{\partial \omega_j}\gamma_{l,k}^{j}(q)\omega_l = f_k, \tag{9}$$

for $k = 3, \ldots, 5$, where

$$f_k = \sum_{i=1}^{2}\frac{\partial \dot{\varphi}_i}{\partial \omega_k}\tau_i. \tag{10}$$

These equations are quite similar in structure to Lagranges' Equations of Motion. However, they differ in the use of velocity coordinates ω_k instead of time derivatives $\dot{q}_j$ and they comprise one additional term that accounts for the nonholonomic constraints. Within the foregoing equation, this is the third term and it contains the so-called Hamel-coefficients $\gamma_{l,k}^{j}$ which are given by

$$\gamma_{l,k}^{j} = \sum_{\nu,\sigma=1}^{n}\left(\frac{\partial^2 \omega_j}{\partial \dot{q}_\nu \partial q_\sigma} - \frac{\partial^2 \omega_j}{\partial \dot{q}_\sigma \partial q_\nu}\right)\frac{\partial \dot{q}_\sigma}{\partial \omega_l}\frac{\partial \dot{q}_\nu}{\partial \omega_k}. \tag{11}$$

Within the derivation, all Hamel coefficients $\gamma_{l,k}^{j}$ vanish except $\gamma_{2,3}^{1}$ and $\gamma_{3,2}^{1}$, which take the values -1 and $+1$, respectively. Hence, the equations of motion of the mobile robot can subsequently be derived as

$$\begin{pmatrix} J_y + m_0 l^2 & m_0 l \cos\alpha & 0 \\ m_0 l \cos\alpha & m_0 + 3m_w & 0 \\ 0 & 0 & J_5 \end{pmatrix} \begin{pmatrix} \dot{\omega}_3 \\ \dot{\omega}_4 \\ \dot{\omega}_5 \end{pmatrix} + \\ + \begin{pmatrix} \frac{1}{2}\left(J_z - J_x - m_0 l^2\right)\omega_5^2 \sin(2\alpha) - m_0 l g \sin\alpha \\ -m_0 l \sin\alpha(\omega_5^2 + \omega_3^2) \\ \left(J_x - J_z + m_0 l^2\right)\omega_3\omega_5 \sin(2\alpha) + m_0 l \omega_4 \omega_5 \sin\alpha \end{pmatrix} = \begin{pmatrix} -1 & -1 \\ \frac{1}{r} & \frac{1}{r} \\ \frac{b}{2r} & -\frac{b}{2r} \end{pmatrix} \begin{pmatrix} \tau_1 \\ \tau_2 \end{pmatrix}. \tag{12}$$

These equations are accompanied by a system of kinematic differential equations which are deduced from the inverse transformation (5) taking the nonholonomic constraints (3) into account:

$$\begin{aligned} \dot{x} &= \cos\left(r\frac{\varphi_1 - \varphi_2}{b}\right)\omega_4, & \dot{y} &= \sin\left(r\frac{\varphi_1 - \varphi_2}{b}\right)\omega_4, & \dot{\alpha} &= \omega_3 \\ \dot{\varphi}_1 &= -\omega_3 + \frac{1}{r}\omega_4 + \frac{b}{2r}\omega_5, & \dot{\varphi}_2 &= -\omega_3 + \frac{1}{r}\omega_4 - \frac{b}{2r}\omega_5. \end{aligned} \tag{13}$$

3. Control Concept

In this section, a controller is presented for the mechanical system described above, which enables the mobile robot to track a given reference trajectory. The controller design is related to the considerations for a similar mechanical system in [6]. In the literature different controller design concepts can be found for the easier problem described in [2, 3], or [4] but also for more complex models as e. g. in [5]. The basic idea of our controller concept is to split the control objective into two tasks. First, the controller has to keep the main body upright, which can be regarded as a stabilization of an inverse pendulum. Second, it has to maintain the position (x, y) of the axle's center point close to a reference trajectory.

The two mentioned control tasks are tackled by a cascade control structure. The outer loop controller solves the tracking control task by commanding appropriate values for the path velocity v and the angular velocity $\dot{\vartheta}$ in order to maintain the axle's center position on the reference trajectory. Hence, it can be regarded as a pure positional controller. The inner loop controller has to fulfill two tasks. It stabilizes the upright body position and controls the actual velocities v and $\dot{\vartheta}$ to meet the commanded velocities from

the outer loop controller. Thus, this part controls the upright position on the one hand and the translational and rotational velocities of the vehicle on the other hand.

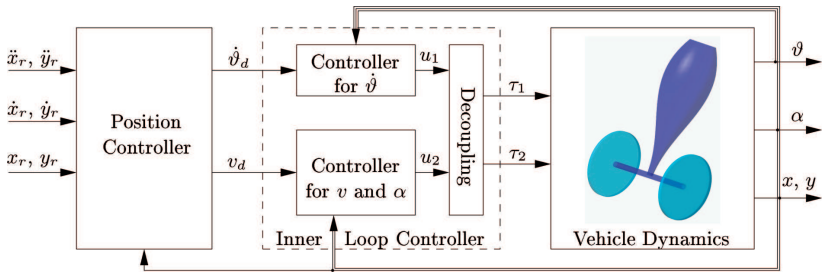

Fig. 2. Overall structure of the controller divided into an inner and an outer loop controller (position controller)

3.1. The outer loop controller

In the first instance, the outer loop controller is based on the assumption that the path velocity v and the angular velocity $\dot{\vartheta}$ can be set arbitrarily. For a given a reference trajectory $\mathcal{P} : t \mapsto (x_r(t), y_r(t))$, we can calculate the reference value for the path velocity v as

$$v_r = \sqrt{\dot{x}_r^2 + \dot{y}_r^2}. \tag{14}$$

As ϑ denotes the angle between the velocity vector of the vehicle's axis' center point and the positive x-axis of the inertial frame, its reference trajectory ϑ_r can be expressed in terms of $\dot{x}_r$ and $\dot{y}_r$ by

$$\vartheta_r = \arctan\left(\frac{\dot{y}_r}{\dot{x}_r}\right). \tag{15}$$

Differentiation with respect to time yields the reference trajectory for the angular velocity

$$\dot{\vartheta}_r = \frac{\dot{x}_r\ddot{y}_r - \ddot{x}_r\dot{y}_r}{\dot{x}_r^2 + \dot{y}_r^2}. \tag{16}$$

As a plausible measure for the tracking error we can introduce the vector $\vec{d}$ between the actual and the reference position of the robot's axle's center point. It can be written in components of the inertial frame $\mathfrak{I}$ as

$$\vec{d} = (x_r - x)\vec{e}_x + (y_r - y)\vec{e}_y \tag{17}$$

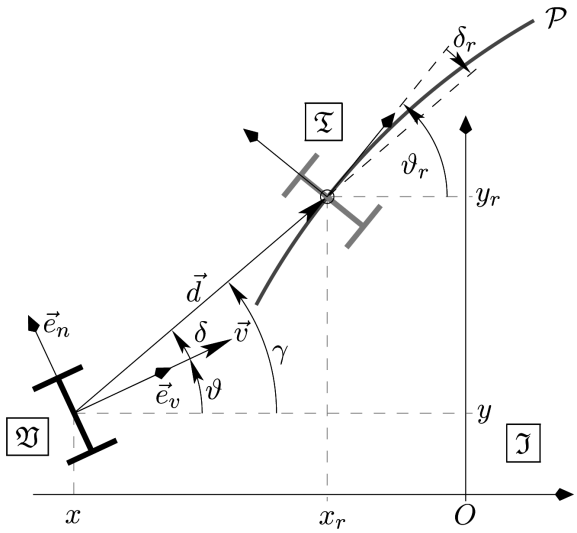

Fig. 3. Actual and reference position of the mobile robot on the reference trajectory $\mathcal{P}$ in view from above

with unit vectors $\vec{e}_x$ and $\vec{e}_y$ in x- and y-direction, respectively. Its absolute value shall be denoted by $d = |\vec{d}|$.

According to Figure 3, we can now define the angles δ and δ_r ($\in [-\pi, \pi)$) between the vector $\vec{d}$ and the actual or the reference driving direction, respectively, from the relations

$$\sin\delta = \frac{\vec{d}\cdot\vec{e}_n}{d}, \qquad \cos\delta = \frac{\vec{d}\cdot\vec{e}_v}{d}, \quad \sin\delta_r = \frac{\vec{d}\cdot\vec{n}_r}{dv_r}, \quad \cos\delta_r = \frac{\vec{d}\cdot\vec{v}_r}{dv_r}, \tag{18}$$

where

$$\vec{v} = \dot{x}\vec{e}_x + \dot{y}\vec{e}_y, \qquad v = |\vec{v}|, \qquad \vec{e}_n = \vec{e}_z \times \vec{e}_v, \qquad \vec{e}_v = \frac{\vec{v}}{v}, \tag{19}$$

and

$$\vec{v}_r = \dot{x}_r\vec{e}_x + \dot{y}_r\vec{e}_y, \qquad v_r = |\vec{v}_r|, \qquad \vec{n}_r = \vec{e}_z \times \vec{v}_r. \tag{20}$$

Therein, vector $\vec{e}_z$ is pointing upwards. For the formulation of the control law, we further need the components d_v and d_n of $\vec{d}$ with respect to the vehicle frame $\mathfrak{V}$, which are defined by

$$\vec{d} = d_v\vec{e}_v + d_n\vec{e}_n \tag{21}$$

and hence are given by

$$d_v = (x_r - x)\cos\vartheta + (y_r - y)\sin\vartheta \quad \text{and} \quad d_n = (x - x_r)\sin\vartheta + (y_r - y)\cos\vartheta. \tag{22}$$

Now, we can formulate some heuristic control objectives. Assuming a large error d, it seems quite reasonable to drive directly in the direction of the error vector $\vec{d}$ in order to reduce the error d as fast as possible. Hence, we might choose the angle δ as an error measure for the control variable $\dot{\vartheta}$ and the absolute distance d as an error measure for the path velocity v.

When d becomes small, the direction of the reference trajectory must also be taken into account for the control of the driving direction. Otherwise the vehicle might cross the reference trajectory in a more obtuse angle, which leads to a sudden change in the error measure δ and might destabilize the controller. Another destabilizing phenomena occurs when the vehicle overtakes the reference trajectory, as it also causes a rapid change in the angle δ. In order to reduce these destabilizing effects, we can introduce the following weighted error measures $\boldsymbol{e} = \begin{pmatrix} e_1 & e_2 & e_3 \end{pmatrix}^{\mathrm{T}}$ with

$$e_1 = w_1(d)\,\mathrm{sgn}(d_v)\,d, \quad e_2 = w_1(d)\sin\delta, \quad \text{and} \quad e_3 = w_2(d)(\delta - \delta_r). \tag{23}$$

Therein, the following functions are defined as

$$w_1(d) = \frac{2}{\pi}\arctan\left(\frac{d}{d_0}\right), \quad w_2(d) = 1 - w_1(d), \text{ and } \mathrm{sgn}(d_v) = \begin{cases} +1 & \text{for } d_v \geq 0 \\ -1 & \text{for } d_v < 0 \end{cases}, \tag{24}$$

where d_0 is a tuning parameter. Note, that the angle $\delta - \delta_r$ is in fact the angle between the reference and the actual driving direction, i. e. $\vartheta_r - \vartheta$.

The desired path velocity v_d and the desired rotational velocity $\dot{\vartheta}_d$ are then calculated as a superposition of the reference values and the proportional feedback of the defined error measures e_i $(i = 1, 2, 3)$:

$$v_d = v_r + a_1 e_1, \qquad \dot{\vartheta}_d = \dot{\vartheta}_r + a_2 e_2 + a_3 e_3. \tag{25}$$

Here, the variables a_i $(i = 1, 2, 3)$ are design parameters of the controller, which have been appropriately chosen. Figure 4 illustrates the described control structure of the outer loop controller.

3.2. The inner loop controller

The inner loop controller has to maintain the actual velocities v and $\dot{\vartheta}$ close to the demanded velocities v_d and $\dot{\vartheta}_d$. Additionally, it has to stabilize the vehicle around its upright position $\alpha = 0$. For the design of the inner loop controller, it has proven helpful to define two new inputs as

$$u_1 = \tau_1 - \tau_2 \qquad \text{and} \qquad u_2 = \tau_1 + \tau_2. \tag{26}$$

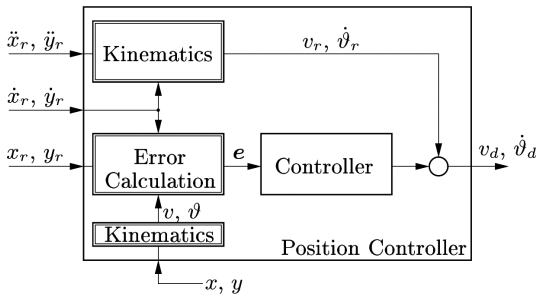

Fig. 4. Outer loop controller acting as a positional controller

Under the assumption that the values of α, $\dot{\alpha}$, and v are measured, the control of $\dot{\vartheta}$ can be regarded as being decoupled from the remaining dynamics (refer to Equation (12)). Choosing

$$u_1 = \frac{r}{2b}\left(J_5 w + \left(J_x - J_z + m_0 l^2\right)\dot{\alpha}\dot{\vartheta}\sin(2\alpha) + m_0 l v \dot{\vartheta}\sin\alpha\right) \tag{27}$$

with some newly introduced input variable w, we can compensate all nonlinearities and reduce the system dynamics to a simple double integrator in ϑ:

$$\ddot{\vartheta} = w. \tag{28}$$

For this linear system we could now design many different stabilizing controllers using linear control theory. For our example we reach sufficiently good tracking performance by setting

$$w = \ddot{\vartheta}_d - k(\dot{\vartheta} - \dot{\vartheta}_d) \tag{29}$$

with some appropiate selection of $k > 0$, as we end up with a stable linear differential equation for the deviation of $\dot{\vartheta}$ from its desired value $\dot{\vartheta}_d$:

$$(\ddot{\vartheta} - \ddot{\vartheta}_d) + k(\dot{\vartheta} - \dot{\vartheta}_d) = 0. \tag{30}$$

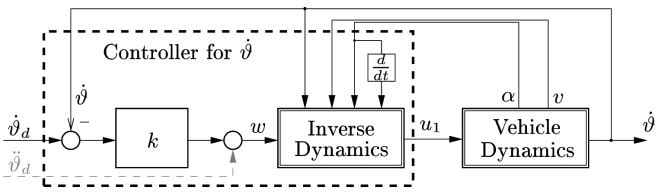

Fig. 5. Controller for the rotational velocity of the vehicle based on an input-output linearized model

Hence, we get a nonlinear controller that is based on an input-output linearization [16] of the vehicle dynamics (refer to Figure 5). If the demanded rotational velocity $\dot{\vartheta}_d$ changes relatively slowly compared to the error

dynamics, one can also additionally neglect the feed forward term that is marked by its gray color in Figure 5.

The remaining dynamics describe the evolution of α and v. For this part, we use a linearization of (12) in the sense of a Taylor approximation of first order around $\alpha, \vartheta \equiv 0$. Thus, we get a linear system of differential equations that is fully decoupled from ϑ:

$$\begin{pmatrix} J_y + m_0 l^2 & m_0 l \\ m_0 l & m_0 + 3m_w \end{pmatrix} \begin{pmatrix} \ddot{\alpha} \\ \dot{v} \end{pmatrix} + \begin{pmatrix} -m_0 l g \alpha \\ 0 \end{pmatrix} = \begin{pmatrix} -1 \\ \frac{1}{r} \end{pmatrix} u_2. \tag{31}$$

On the basis of these equations, we can now design a stabilizing linear controller. Assuming a relatively small rate of change in the demanded velocity v_d from the outer loop controller, it has proven sufficient to design a set point controller rather than a tracking controller not only for the control of the upright body position α but also for the desired path velocity v (see Figure 6).

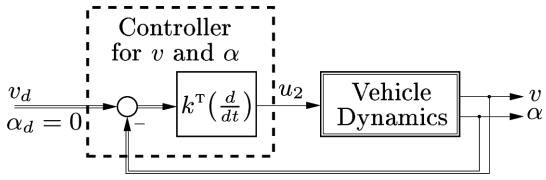

Fig. 6. SIMO control structure of the inner loop controller for α and v

As we want to place the roots of the linear closed loop system arbitrarily with the help of a static feedback controller, we choose the following control law for the input signal u_2:

$$u_2 = -\underbrace{\left(k_{10} + k_{11}\frac{d}{dt}() \quad k_{20}\right)}_{k^{\mathrm{T}}(\frac{d}{dt})} \begin{pmatrix} \alpha \\ v_d - v \end{pmatrix} = -k_{11}\dot{\alpha} - k_{10}\alpha + k_{20}(v_d - v) \tag{32}$$

comprising the parameters k_{11}, k_{10}, and k_{20}. Consequently, we get the characteristic polynomial of the closed loop system

$$c_3 s^3 + (c_1 k_{11} + c_2 k_{20}) s^2 + (d_1 + c_1 k_{10}) s + c_0 k_{20} = 0 \tag{33}$$

where

$$c_0 = -m_0 l g, \qquad c_1 = -(m_0 l + (m_0 + 3m_w) r), \tag{34}$$

$$c_2 = (J_y + m_0 l^2 + m_0 l r), \qquad c_3 = ((J_y + m_0 l^2)(m_0 + 3m_w) - (m_0 l)^2) r, \tag{35}$$

and

$$d_1 = -m_0 l g r (m_0 + 3m_w). \tag{36}$$

By comparing these coefficients with the coefficients of the desired closed loop characteristic polynomial

$$s^3 + l_2 s^2 + l_1 s + l_0 = 0, \tag{37}$$

we are led to an affine system of equations in the controller parameters k_{10}, k_{11}, and k_{20}:

$$\begin{pmatrix} l_2 \\ l_1 \\ l_0 \end{pmatrix} = \begin{pmatrix} 0 & \frac{c_1}{c_3} & \frac{c_2}{c_3} \\ \frac{c_1}{c_3} & 0 & 0 \\ 0 & 0 & \frac{c_0}{c_3} \end{pmatrix} \begin{pmatrix} k_{10} \\ k_{11} \\ k_{20} \end{pmatrix} + \begin{pmatrix} 0 \\ \frac{d_1}{c_3} \\ 0 \end{pmatrix} \tag{38}$$

with the unique solution

$$k_{10} = \frac{c_3 l_1 - d_1}{c_1}, \qquad k_{11} = \frac{c_3(c_0 l_2 - c_2 l_0)}{c_0 c_1}, \quad \text{and} \quad k_{20} = \frac{c_3 l_0}{c_0}. \tag{39}$$

To ensure stability, the inner loop controller has been parametrized to be significantly faster than the outer controller. Moreover, this assumption helps to justify the set point controller and hence to drastically reduce the complexity of the inner loop controller. Even if no stability proof can be provided for the presented controller, it has shown good performance in simulation studies (see e. g. the following section).

4. Simulation Results

Within this section some examples are presented that illustrate the performance of the previously designed controller. All models were formulated using the modeling language Modelica and were simulated in Dymola.

As a first example, the tracking performance of the controlled vehicle is demonstrated for a circular reference trajectory. The initial position of the vehicle is given by

$$x_0 = 0.5 \qquad \text{and} \qquad y_0 = 0.5, \tag{40}$$

which results in an initial positional error (see Figure 7). The initial driving direction is parallel to the inertial x-axis, i. e. $\vartheta_0 = 0$. The simulation results are plotted in Figures 7, 8, and 9.

After a short correction phase, the vehicle follows the given reference trajectory sufficiently well. This can be seen either for the coordinates x and y in Figure 7 or for the path velocity v and the angle ϑ in Figure 8. The

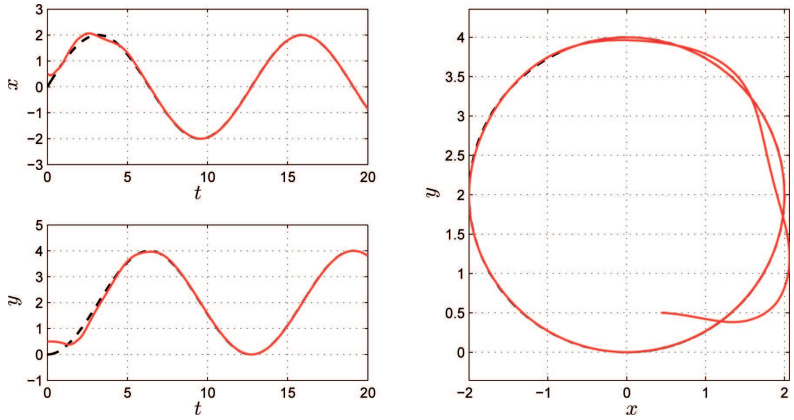

Fig. 7. Actual (red solid line) and circular reference trajectory (black dashed line) of x and y for an initial displacement

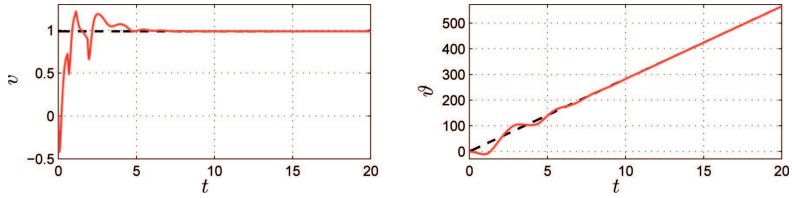

Fig. 8. Actual (red solid line) and reference trajectory (black dashed line) of v and ϑ (in degree) for an initial displacement from the circular reference trajectory in x, y

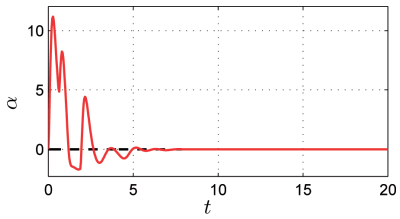

Fig. 9. Trajectory (red solid line) and reference value (black dashed line) of angle α (in degree) for an initial displacement from the circular reference trajectory in x, y

position controller for α does also show quite good performance (refer to Figure 9) as it keeps the body upright with a maximum decline of 11°.

The second example shows the tracking performance of the controller on a straight reference trajectory for an initial positional and rotational error (see Figure 10). The initial position and driving direction of the vehicle is given by

$$x_0 = 1, \qquad y_0 = 0, \qquad \text{and} \qquad \vartheta_0 = 0. \tag{41}$$

Figures 10, 11, and 12 show the simulation results. At the beginning of the simulation, one can see the action of the coupled v- and α-controller.

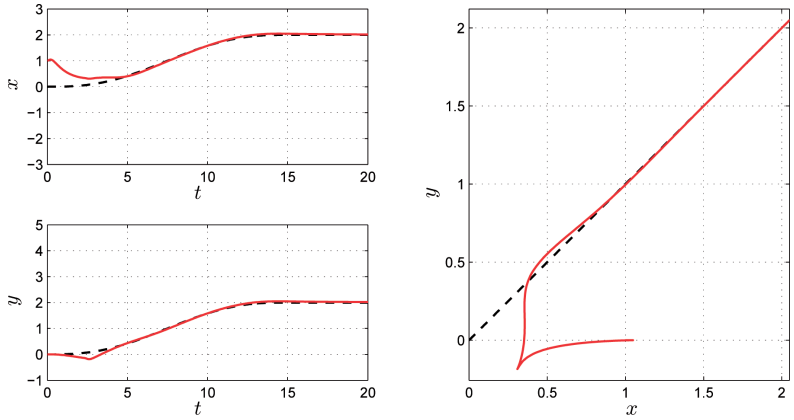

Fig. 10. Actual (red solid line) and straight reference trajectory (black dashed line) of x and y for an initial positional and rotational error

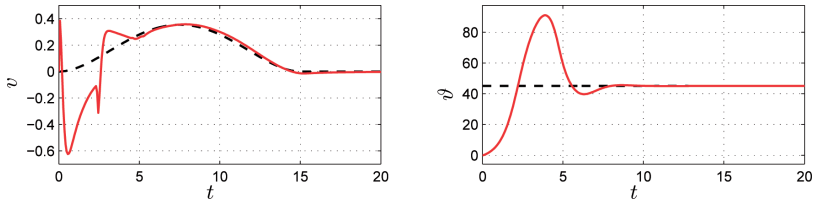

Fig. 11. Actual (red solid line) and reference trajectory (black dashed line) of v and ϑ (in degree) for an initial positional and rotational deviation from the straight reference trajectory in x and y

In order to accelerate the vehicle in the appropriate direction, the controller moves the axle's center point in the other direction. As a reaction the body tilts and creates a torque around the wheels' axis. By compensating this torque the vehicle begins to move in the intended direction. Here, the vehicle moves backwards due to the initial positional error. After a short period it stops and changes the direction of its motion in order to follow the reference trajectory. In the following period, the vehicle approaches the reference trajectory (black dashed line in Figures 10 and 11) showing the good performance of the ϑ-controller as well as the controller for v.

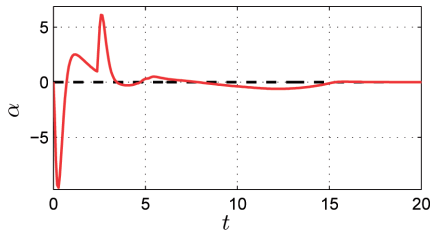

Fig. 12. Trajectory (red solid line) and reference value (black dashed line) of angle α (in degree) for an initial positional and rotational deviation from the straight reference trajectory in x and y

Figure 12 depicts the trajectory of the tilting angle α of the main body. As the maximum absolute tilting angle is smaller than 10 degrees, the position controller also shows sufficiently good performance.

5. Conclusions

This paper presents a control concept for a mobile robot rolling on the horizontal plane. After introducing the nonholonomic mechanical system, a mathematical model has been derived using Hamel's equations of motion [1]. With the help of a cascade control structure, a tracking controller has been designed that tracks the mobile robot along a given reference trajectory in an upright position. While, the outer loop controller solves the tracking control task for the kinematic wheel model by commanding appropriate values for both the path velocity and the angular velocity, the inner loop controller stabilizes the upright body position and maintains the commanded velocities from the outer loop controller. Exploiting the inner structure of the equations of motion, the inner loop controller has been split into two separate controllers. For the dynamics of the angular velocity a linearizing control law has been presented. For the remaining dynamics a linear set-point control law has been designed. Finally, the performance of the implemented tracking control law has been illustrated by simulation results.

Manuscript received by Editorial Board, December 16, 2013;
final version, April 19, 2014.

REFERENCES

[1] Hamel G.: Über die virtuellen Verschiebungen in der Mechanik. *Mathematische Annalen*, 59, 416-434, 1904.
[2] Kim B. M., and Tsiotras P.: Controllers for unicycle-type wheeled robots: Theoretical results and experimental validation. *IEEE Trans. on Robotics and Automation*, 18(3), 294-307, June 2002.
[3] Lee T.-Ch., Song K.-T., Lee Ch.-H., and Teng Ch.-Ch.: Tracking control of unicycle-modeled mobile robots using a saturation feedback controller. *IEEE TRANSACTIONS ON CONTROL SYSTEMS TECHNOLOGY*, 9(2), 305-328, March 2001.
[4] M'Closkey R.T., and Murray R.M.: Exponential stabilization of driftless nonlinear control systems using homogeneous feedback. *TAC*, 42(5), 614-628, 1997.
[5] Sharp R. S.: On the stability and control of unicycles. In *Proc. R. Soc. A*, 2010.
[6] Franke M., Rudolph J., and Woittennek F.: Motion planning and feedback control of a planar robotic unicycle model. In *Proc. Int. Conf. on Methods and Models in Automation and Robotics*, volume 14, 2009.
[7] Franke M., Zaiczek T., and Röbenack K.: Simulation of nonholonomic mechanical systems using algorithmic differentiation. In *Proc. 7th Vienna International Conference on Mathematical Modelling (MATHMOD)*, 2012.
[8] Goldstein H.: *Classical Mechanics*. Addison-Wesley series in physics. Addison-Wesley Pub. Co., 1980.

[9] Neimark I. I., and Fufaev N. A.: *Dynamics of Nonholonomic Systems*. American Mathemtical Society, 1972.
[10] Griepentrog E., and März R.: *Differential-Algebraic Equations and Their Numerical Treatment*, volume 88. Teubner Verlagsgesellschaft, Leipzig, 1986.
[11] Brenan K. E., Campbell S. L., and Petzold L. R.: *Numerical Solution of Initial-Value Problems in Differential-Algebraic Equations*. SIAM, Philadelphia, 2nd edition, 1996.
[12] Röbenack K., Bausch T., and Uhlig A.: Struktureller Index von Deskriptorvariablen. In Klaus Panreck and Frank Dörrscheidt, editors, *Simulationstechnik, 15. Symposium in Paderborn, ASIM 2001*, Frontiers in Simulation, pages 569-574. SCS – The Society for Modeling and Simulation International, 2001.
[13] Kunkel P., and Mehrmann V.: *Differential-Algebraic Equations: Analysis and Numerical Solution*. EMS Publishing House, Zürich, 2006.
[14] Cameron J.M., and Book W.J.: Modeling mechanisms with nonholonomic joints using the Boltzmann-Hamel equations. *International Journal of Robotics Research*, 16(1), 47-59, February 1997.
[15] Jarzebowska E., and Lewandowski R.: Modeling and control design using the Boltzmann-Hamel equations: A roller-racer example. In *Proc. 8th IFAC Symposium on Robot Control*, pages 236-241, 2006.
[16] Isidori A.: *Nonlinear Control Systems*. Springer, 3. edition, 1995.

Sterowanie śledzące robota zachowującego równowagę – podejście oparte na modelu

S t r e s z c z e n i e

W artykule przedstawiono koncepcję sterowania ruchem jednoosiowego robota poruszającego się po płaszczyźnie poziomej. Model matematyczny nieholonomicznego systemu mechanicznego wyprowadzono korzystając z równań ruchu Hamela. Opisano następnie szczegółowo koncepcję sterownika śledzącego. Sterownik prowadzi poruszający się robot po zadanej trajektorii utrzymując go jednocześnie w pozycji pionowej. Cel sterowania jest osiągnięty przy zastosowaniu kaskadowej struktury sterowania. Dzięki odpowiedniej transformacji danych wejściowych, w podsystemie istnieje możliwość linearyzacji wejście-wyjście. Dla dynamiki pozostałej części zaprezentowano prawo liniowego sterowania stałowartościowego. Ostatecznie, jakość działania zastosowanych praw sterowania zilustrowano wynikami symulacji.